Supplementary Materials of: Structural control energy of resting-state functional brain states reveals less cost-effective brain dynamics in psychosis vulnerability.

Daniela Zöller[a,b,d,c], Corrado Sandini[d], Marie Schaer[d], Stephan Eliez[d], Danielle S. Bassett[e,f,g,h,i], Dimitri Van De Ville[a,b]

[a] *Medical Image Processing Laboratory, Institute of Bioengineering, École Polytechnique Fédérale de Lausanne (EPFL), Lausanne, Switzerland*
[b] *Department of Radiology and Medical Informatics, University of Geneva, Geneva, Switzerland*
[c] *Institute of Neuromodulation and Neurotechnology, Department of Neurosurgery and Neurotechnology, University of Tübingen*
[d] *Developmental Imaging an Psychopathology Laboratory, Department of Psychiatry, University of Geneva, Geneva, Switzerland*
[e] *Department of Bioengineering, University of Pennsylvania, Philadelphia, PA, United States*
[f] *Department of Electrical & Systems Engineering, University of Pennsylvania, Philadelphia, PA, United States*
[g] *Department of Neurology, University of Pennsylvania, Philadelphia, PA, United States*
[h] *Department of Physics & Astronomy, University of Pennsylvania, Philadelphia, PA, United States*
[i] *Department of Psychiatry, University of Pennsylvania, Philadelphia, PA, United States*

Contents

*Corresponding author
Email address: daniela.zoeller@uni-tuebingen.de (Daniela Zöller)

Supplementary figures

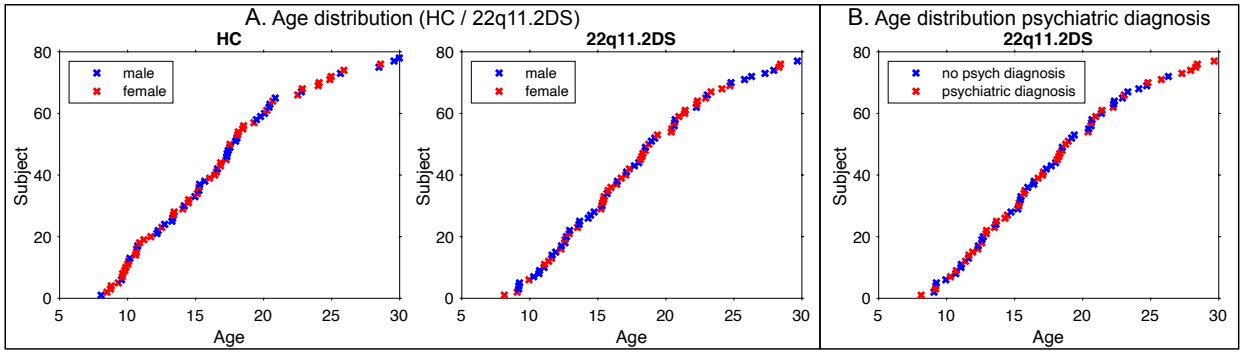

Figure S1: Distribution of all subjects over age for A) HCs and patients with 22q11.2DS, as well as B) for patients with 22q11.2DS with and without any psychiatric disorder. Patients with psychiatric diagnoses are well distributed throughout the age range. The age in patients with psychiatric disorders (17.47 ± 5.85 years) and in patients without any psychiatric diagnosis (16.93 ± 4.84) does not significantly differ ($p = 0.66$).

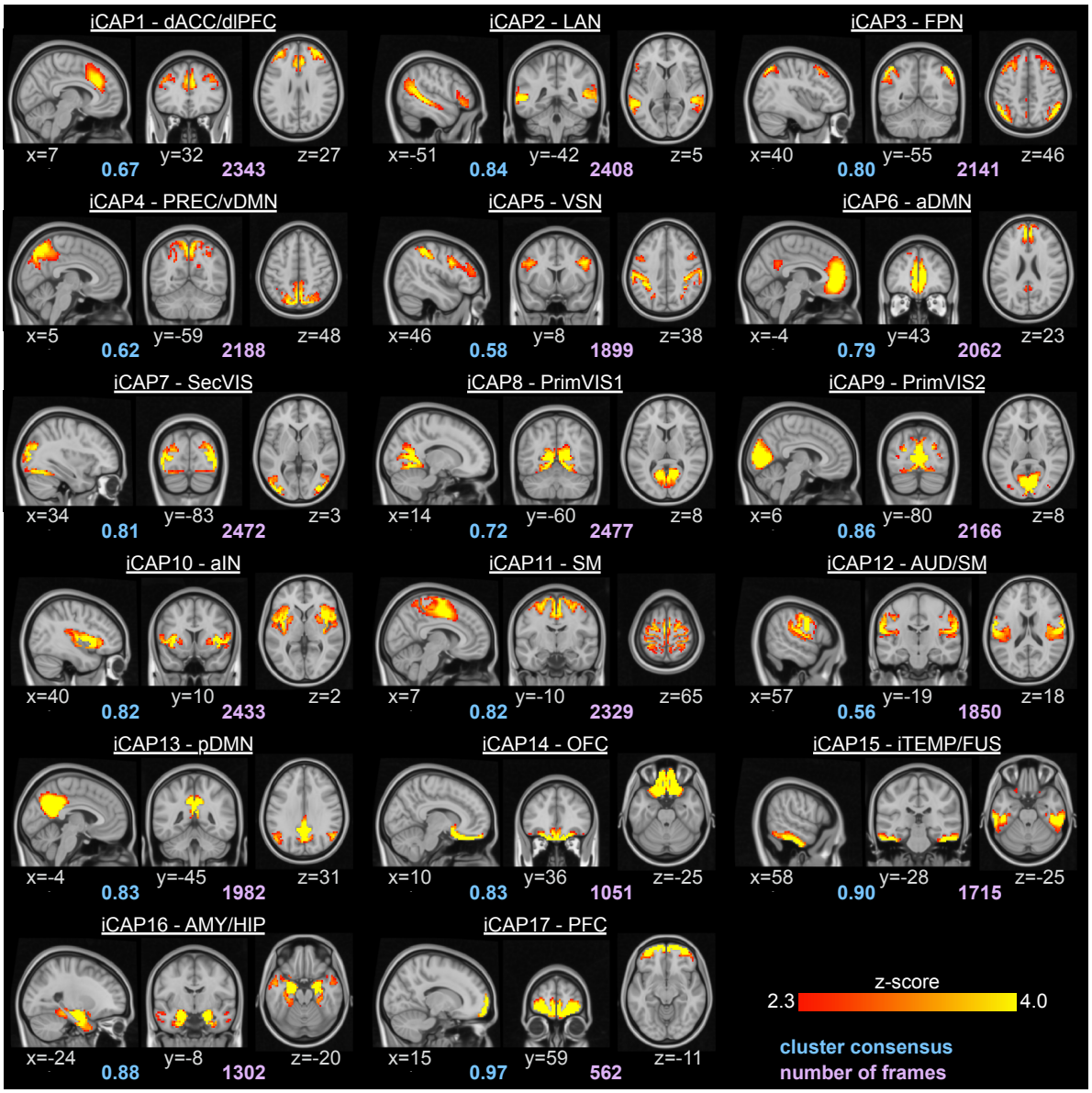

Figure S2: Spatial patterns of the 17 iCAPs retrieved from all subjects, including both HCs and patients with 22q11DS. The locations denote displayed slices in MNI coordinates. Blue values denote the average consensus of each cluster, purple values indicate the total number of innovation frames that were assigned to this cluster. Maps are identical to the ones in (Zöller et al., 2019), sorted according to the activation duration in HCs. dACC/dlPFC – dorsal anterior cingulate cortex / dorsolateral prefrontal cortex, LAN – language network, FPN – fronto-parietal network, PREC/vDMN – precuneus/ventral DMN, VSN – visuospatial network, aDMN – anterior DMN, SecVIS – secondary visual, PrimVIS1 – primary visual 1, PrimVIS2 – primary visual 2, aIN – anterior insula, SM – sensorimotor, AUD/SM – auditory/sensorimotor, pDMN – posterior DMN, OFC – orbitofrontal cortex, iTEMP/FUS –inferior temporal/fusiform, AMY/HIP – amygdala/hippocampus, PFC – prefrontal cortex.

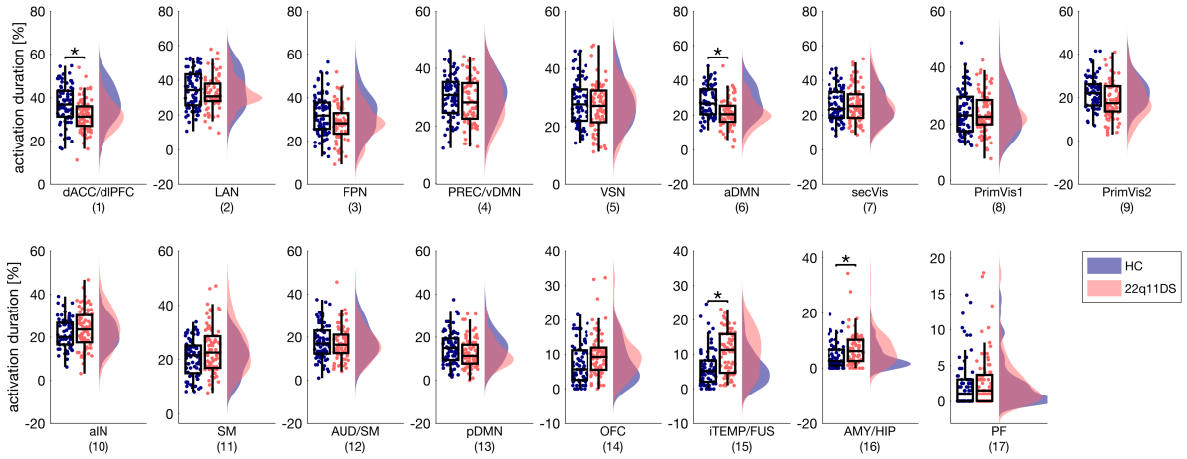

Figure S3: Statistics of total temporal duration for each iCAP. P-values are corrected for multiple comparisons based on permutation testing (Westfall and Young, 1993); age, sex and FSIQ were included as covariates. Significant group differences ($p<0.05$) were marked with an asterisk. Scatterplots represent the single-subject duration measures. Results are identical to those in (Zöller et al., 2019), but sorted according to the activation duration in HCs, and with alternative correction for multiple comparisons. All p-values and T-statistics can be found in supplementary table S3.

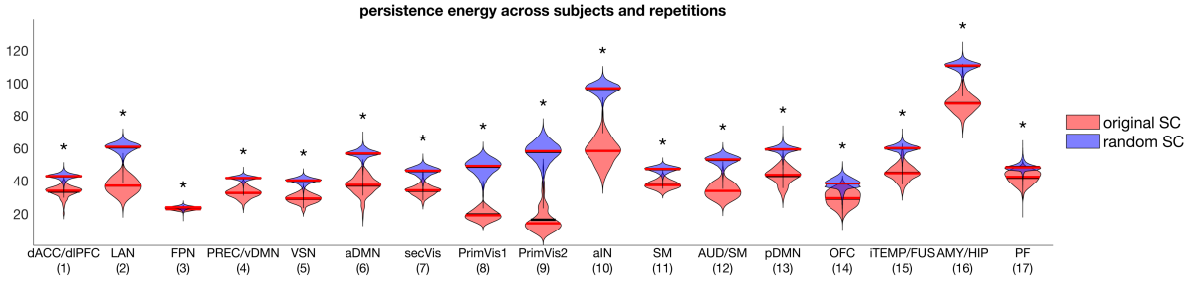

Figure S4: For each subject, persistence energy was computed for 100 random null models that preserve the subject's structural network topology (Rubinov and Sporns, 2010). The brain state spatial maps $\mathbf{x}_k$ were preserved. The blue violin plots show the distribution of persistence energy values across the 100 repetitions and 155 subjects. The red violin plots show the original persistence energy of the 155 subjects. Comparisons were done by fitting a linear mixed effect model to the difference between the true persistence energy value of a subject and the persistence energy computed for randomized structural connectomes. Permutation rounds were modeled as random effects in the mixed model. P-values were corrected for multiple comparisons using Bonferroni correction. Significant group differences ($p<0.05$) were marked with an asterisk. All p-values and T-statistics can be found in table S7.

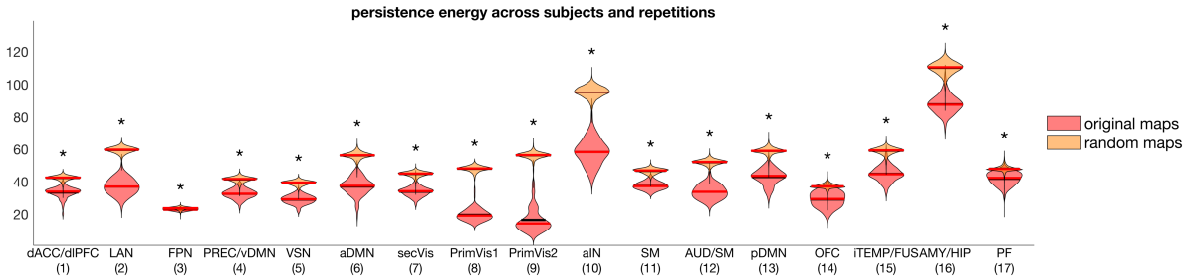

Figure S5: For each subject, persistence energy was computed pertaining the subject's structural connectivity, and 100 times randomly shuffling the iCAPs maps (random permutations of brain regions). Randomized brain state vectors $\mathbf{x}_k$ were created for each iCAP k by randomly permuting the regional activation values for that brain state. The structural connectomes for each individual were preserved. The orange violin plots show the distribution of persistence energy values across the 100 repetitions and 155 subjects. The red violin plots show the original persistence energy of the 155 subjects. Comparisons were done by fitting a linear mixed effect model to the difference between the true persistence energy value of a subject and the persistence energy computed for randomized brain states. Permutation rounds were modeled as random effects in the mixed model. P-values were corrected for multiple comparisons using Bonferroni correction. Significant group differences ($p<0.05$) were marked with an asterisk. All p-values and T-statistics can be found in table S5.

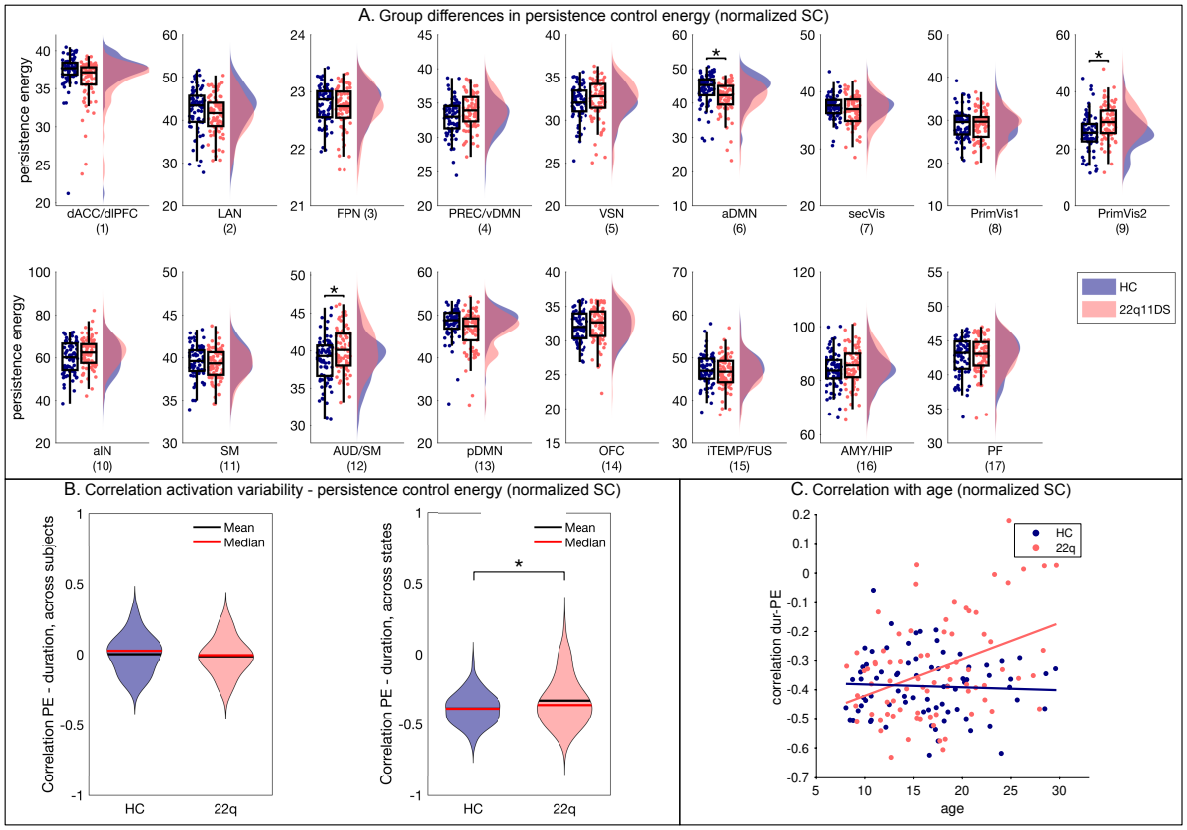

Figure S6: Analysis of persistence control energy for normalized structural connectivity (streamline counts divided by the relative volume of each brain region). A) The pattern of group differences in persistence control energy resembles those for non-normalized structural connectivity (figure 1 of main manuscript). p-values and T-statistics can be found in supplementary table S6. B) The correlation between activation duration and persistence control energy resembles the results for non-normalized structural connectivity. Across subjects, the correlation is not significantly different (left, p = 0.741, T = -0.33). Across subjects, there is a significant negative correlation, which is more pronounced in HCs than in patients with 22q11.2DS (p = 0.028, T = -2.22) C) Similarly as for non-normalized structural connectivity, this correlation between activation duration and persistence control energy becomes more pronounced with age in patients (c = 0.39, p ¡ 0.001), but unchanged with age in HCs (c = -0.06, p = 0.619).

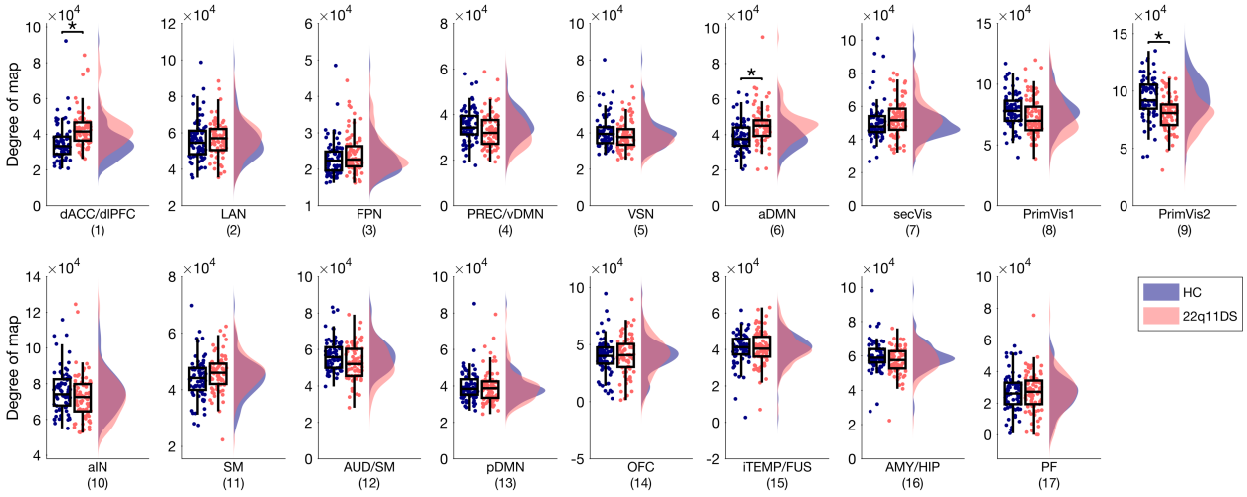

Figure S7: Group differences in degree (total streamline count per region) of the 17 functional brain states in patients with 22q11DS compared to HCs. Degree $d_{iCAP,k}$ of each brain state k was calculated as the sum of weighted degree d_n in region n, multiplied by the iCAP's regional map $\mathbf{x}_k$ ($d_{iCAP,k} = \sum_{n=1}^{N_reg} d_n * x_{k,n}$, with N_{reg} the number of brain regions, d_n the degree of the region, and $x_{k,n}$ the value iCAP k in region n). P-values are corrected for multiple comparisons based on permutation testing (Westfall and Young, 1993); age, sex and FSIQ were included as covariates. Significant group differences ($p<0.05$) are marked with an asterisk. The results show that group differences in degree are significant in dACC/dlPFC, aDMN, and PrimVis2. All three of these brain states have also significantly altered persistence control energy (see figure 1 of the main manuscript), which is expected, due to the close relationship between persistence energy and weighted degree in whole-brain control problems (Karrer et al., 2019). All p-values and T-statistics can be found in supplementary table S7.

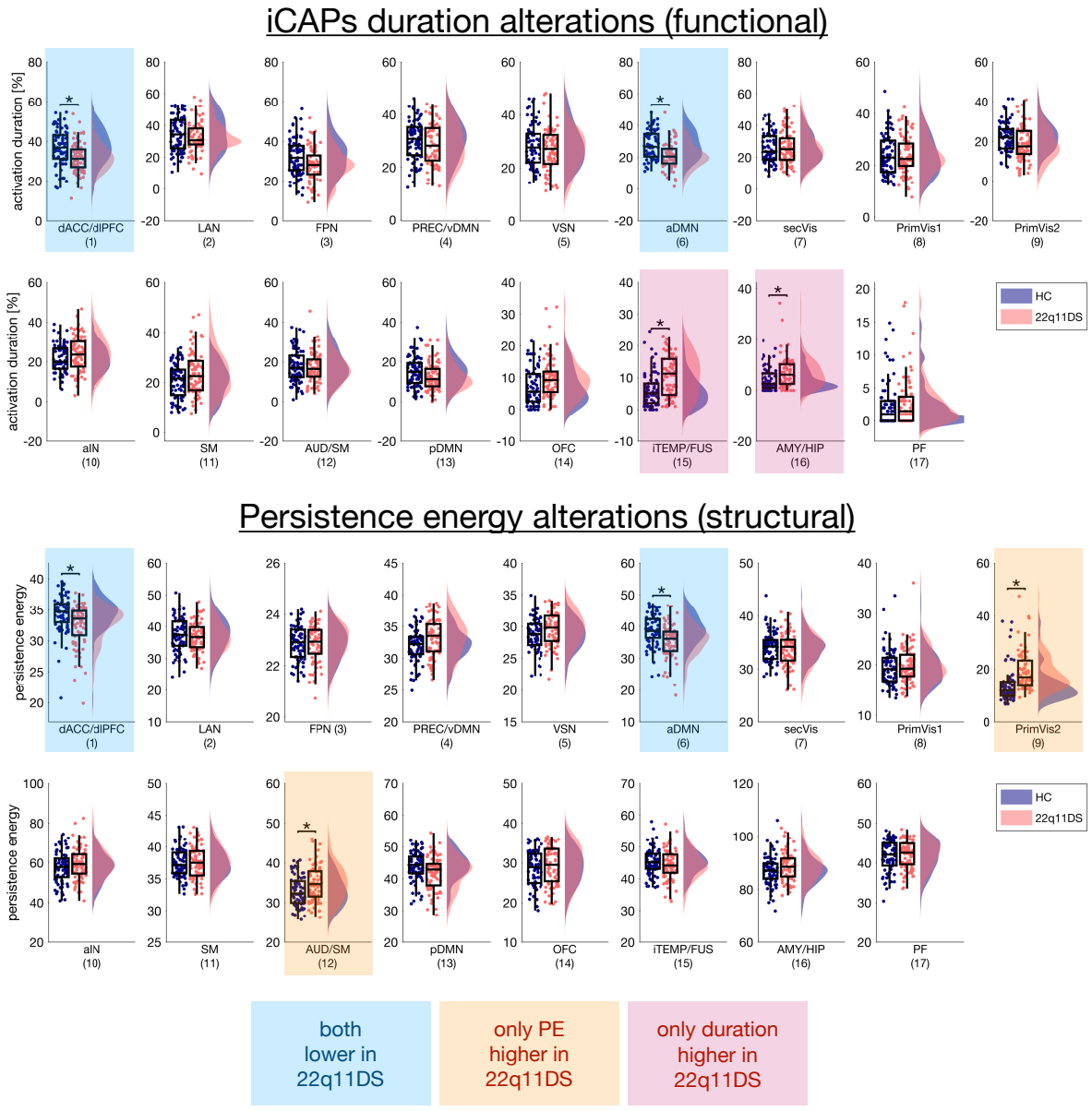

Figure S8: Comparison of alterations in resting-state activation duration (supplementary figure S3) and structural persistence control energy (figure 1 of main manuscript). P-values are corrected for multiple comparisons based on permutation testing (Westfall and Young, 1993). Significant group differences ($p<0.05$) were marked with an asterisk. Scatterplots represent the single-subject duration measures. While there were alterations in both modalities, there was no clear pattern of common alterations.

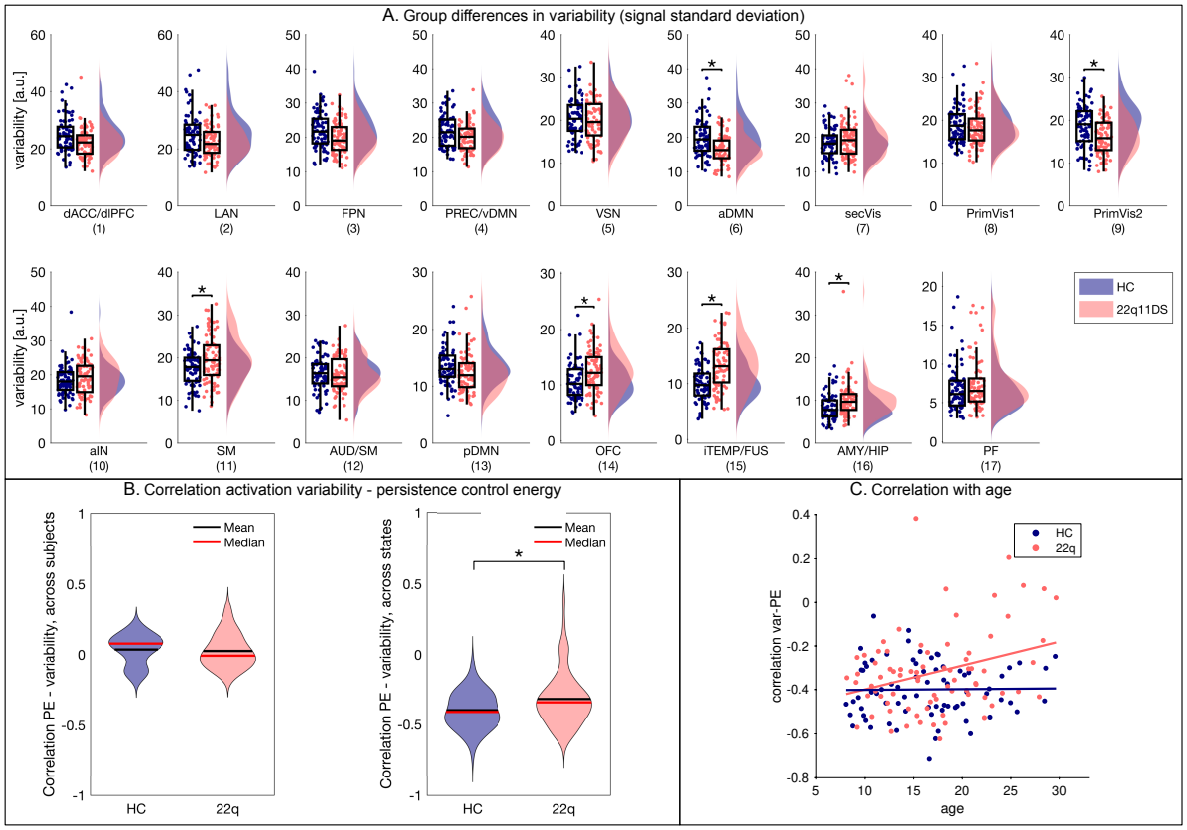

Figure S9: Analysis of temporal variability (i.e., the standard deviation of each iCAP's time course) and its relationship with persistence control energy. A) Group differences in activation variability resemble group differences in activation duration (supplementary figure S3). p-values and T-statistics can be found in table S8. B) The correlation between activation variability and persistence control energy resembles the results for activation duration. Across subjects, the correlation is not significantly different (left, p = 0.782, T = -0.27). Across subjects, there is a significant negative correlation, which is more pronounced in HCs than in patients with 22q11.2DS (p = 0.003, T = -3.00) C) Similarly as for activation duration, this correlation between variability and persistence control energy becomes more pronounced with age in patients (c = 0.29, p = 0.010), but unchanged with age in HCs (c = 0.04, p = 0.729).

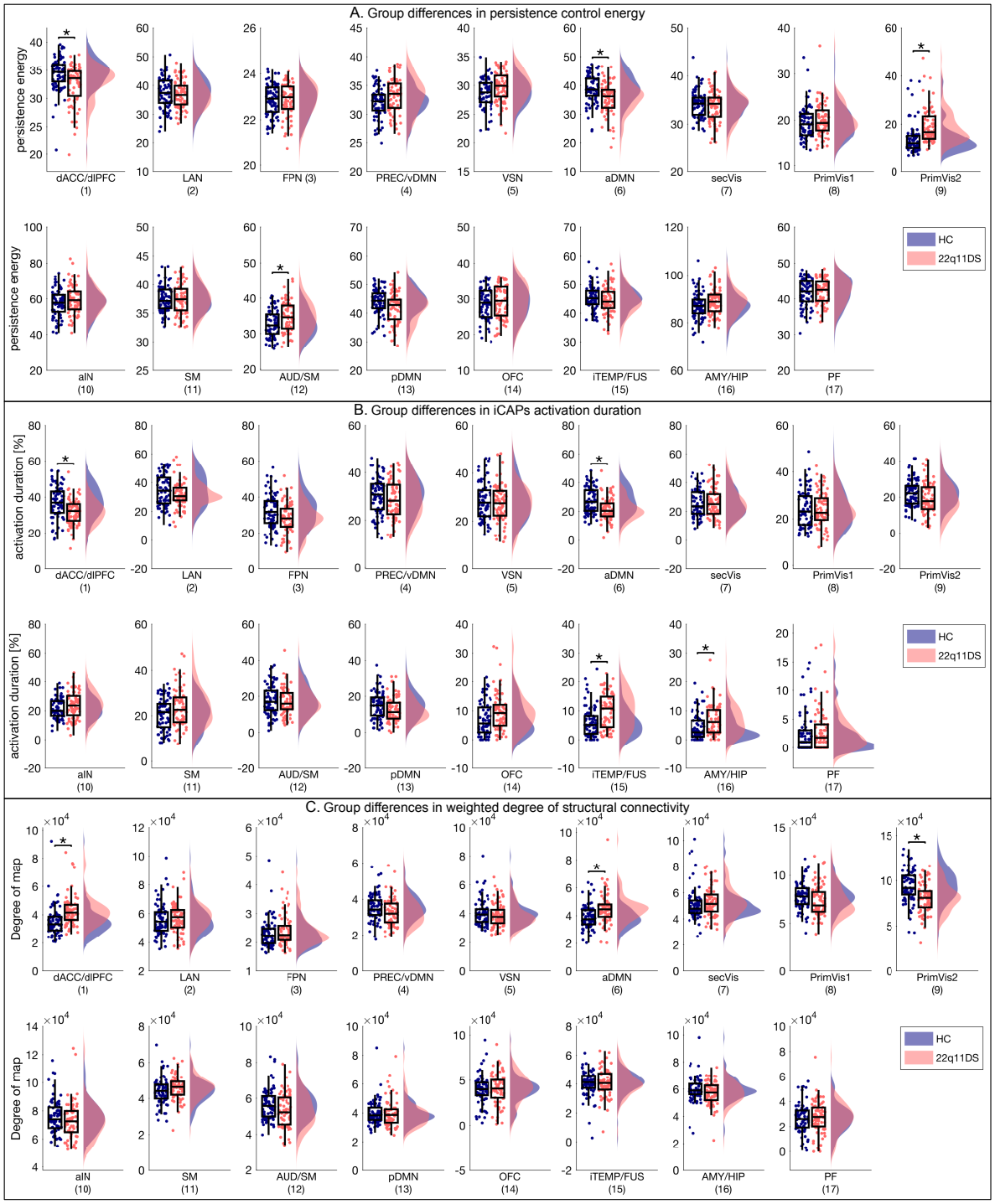

Figure S10: Group comparison results excluding the five subjects with a diagnosis of schizophrenia or schizoaffective disorder. A) Group differences in persistence control energy (as in figure 1 of the main manuscript). B) Group differences in iCAPs activation duration (as in supplementary figure S3). C) Group differences in weighted degree of structural connectivity (as in supplementary figure S7). For all three measures, excluding the five participants with psychosis does not change the overall results.

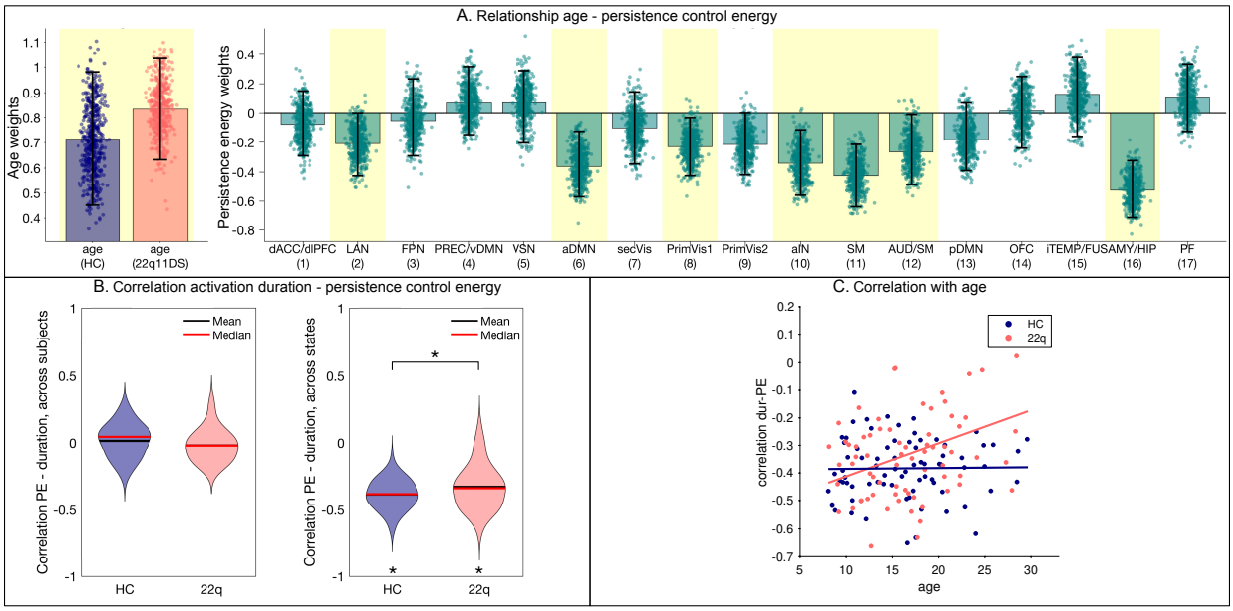

Figure S11: Relationship with age and correlation between persistence control energy and activation duration excluding the five subjects with a diagnosis of schizophrenia or schizoaffective disorder. A) Relationship of persistence control energy and age analyzed with PLS (as in figure 2 of the main manuscript). There remains one significant correlation component (pj0.001). In comparison with the original results, the effect in pDMN became weaker, while the effect in AUD/SM became stronger, resulting in an identical number of 7 stable age effects out of 17 states. Error bars indicate bootstrapping 95% confidence intervals; stable results are indicated by yellow background. B) Relationship between persistence control energy and activation duration across subjects (left, p = 0.499, T = -0.69) and across states (right, p = 0.015, T = 2.46) (as in figure 3 of the main manuscript). C) Relationship of the energy-age duration with age (as in figure 4 of the main manuscript). Correlation in healthy controls (HCs): c = 0.01, p = 0.929; correlation in 22q11.2DS: c = 0.37, p = 0.002. Overall all results remain similar when patients with psychosis are excluded from the analysis.

Supplementary tables

Table S1: Test statistics corresponding to figure 1 of the main manuscript: Results from two-sample t-tests comparing persistence control energy of each iCAP between HCs and patients with 22q11DS. Age, gender and FSIQ were included as nuisance regressors. P-values were corrected for multiple comparisons based on permutation testing (Westfall and Young, 1993).

iCAP	t-statistic	p-value	effect size (Cohen's d)
dACC/dlPFC (1)	3.56	0.007	0.58
LAN (2)	0.67	1.000	0.11
FPN (3)	0.07	1.000	-0.01
PREC/vDMN (4)	2.70	0.113	-0.44
VSN (5)	2.26	0.326	-0.37
aDMN (6)	3.92	0.002	0.64
secVis (7)	0.87	0.999	0.14
PrimVis1 (8)	1.11	0.991	-0.18
PrimVis2 (9)	4.83	0.000	-0.79
aIN (10)	1.68	0.770	-0.27
SM (11)	0.49	1.000	-0.08
AUD/SM (12)	3.26	0.020	-0.53
pDMN (13)	2.44	0.219	0.40
OFC (14)	0.85	0.999	-0.14
iTEMP/FUS (15)	1.24	0.973	0.20
AMY/HIP (16)	2.46	0.209	-0.40
PF (17)	0.55	1.000	-0.09

Table S2: Bootstrap data corresponding to figure 2 of the main manuscript: PLSC results from testing for the relationship between persistence control energy and age. The table shows bootstrap mean and the 95% confidence interval upper (97.5%) and lower (2.5%) bounds of age weights and brain weights.

Weights type	item	bootstrap mean	boostrap 2.5th percentile	bootstrap 97.5th percentile
Age	HC	0.57	0.380	0.87
	22q11DS	0.82	0.699	1.11
iCAP persistence control energy	dACC/dlPFC (1)	-0.08	-0.286	0.15
	LAN (2)	-0.21	-0.409	-0.02
	FPN (3)	-0.01	-0.248	0.23
	PREC/vDMN (4)	0.09	-0.135	0.35
	VSN (5)	-0.05	-0.298	0.20
	aDMN (6)	-0.35	-0.572	-0.11
	secVis (7)	-0.16	-0.375	0.05
	PrimVis1 (8)	-0.23	-0.410	-0.02
	PrimVis2 (9)	-0.17	-0.370	0.04
	aIN (10)	-0.36	-0.589	-0.12
	SM (11)	-0.37	-0.557	-0.17
	AUD/SM (12)	-0.19	-0.421	0.04
	pDMN (13)	-0.23	-0.450	-0.01
	OFC (14)	0.09	-0.168	0.36
	iTEMP/FUS (15)	0.15	-0.113	0.39
	AMY/HIP (16)	-0.54	-0.731	-0.35
	PF (17)	0.18	-0.074	0.42

Table S3: Test statistics corresponding to supplementary figure S3: Results from two-sample t-tests comparing activation duration of each iCAP between HCs and patients with 22q11DS. Age, gender and FSIQ were included as nuisance regressors. P-values were corrected for multiple comparisons based on permutation testing (Westfall and Young, 1993).

iCAP	t-statistic	p-value	effect size (Cohen's d)
dACC/dlPFC (1)	3.91	0.004	0.64
LAN (2)	1.56	0.874	0.25
FPN (3)	2.92	0.064	0.48
PREC/vDMN (4)	1.11	0.992	0.18
VSN (5)	0.91	1.000	0.15
aDMN (6)	5.28	0.000	0.86
secVis (7)	0.24	1.000	-0.04
PrimVis1 (8)	0.12	1.000	0.02
PrimVis2 (9)	2.64	0.134	0.43
aIN (10)	1.47	0.915	-0.24
SM (11)	2.68	0.118	-0.44
AUD/SM (12)	0.86	1.000	0.14
pDMN (13)	2.35	0.279	0.38
OFC (14)	2.54	0.172	-0.41
iTEMP/FUS (15)	4.83	0.000	-0.79
AMY/HIP (16)	3.07	0.040	-0.50
PF (17)	0.73	1.000	-0.12

Table S4: Test statistics corresponding to supplementary figure S4: Results from comparisons between persistence control energy computed based on original structural connectivity and based on randomized structural connectivity. The original iCAPs spatial maps were kept intact for this analysis. For statistics, we used mixed models regression analysis modeling each permutation as random effect. P-values were corrected for multiple comparisons using Bonferroni correction.

iCAP	T-statistic	p-value
dACC/dlPFC (1)	33.73	0.000
LAN (2)	55.76	0.000
FPN (3)	15.16	0.000
PREC/vDMN (4)	36.92	0.000
VSN (5)	47.29	0.000
aDMN (6)	44.14	0.000
secVis (7)	45.83	0.000
PrimVis1 (8)	96.24	0.000
PrimVis2 (9)	66.41	0.000
aIN (10)	57.94	0.000
SM (11)	48.01	0.000
AUD/SM (12)	51.84	0.000
pDMN (13)	39.42	0.000
OFC (14)	21.98	0.000
iTEMP/FUS (15)	39.18	0.000
AMY/HIP (16)	48.71	0.000
PF (17)	19.89	0.000

Table S5: Test statistics corresponding to supplementary figure S5: Results from comparisons between persistence control energy computed based on original brain states and based on randomized iCAPs spatial maps. The original structural connectivity matrices were kept intact for this analysis. For statistics, we used mixed models regression analysis modeling each permutation as random effect. P-values were corrected for multiple comparisons using Bonferroni correction.

iCAP	T-statistic	p-value
dACC/dlPFC (1)	32.82	0.000
LAN (2)	56.16	0.000
FPN (3)	17.24	0.000
PREC/vDMN (4)	37.02	0.000
VSN (5)	47.49	0.000
aDMN (6)	42.91	0.000
secVis (7)	47.83	0.000
PrimVis1 (8)	92.65	0.000
PrimVis2 (9)	62.72	0.000
aIN (10)	59.69	0.000
SM (11)	48.25	0.000
AUD/SM (12)	51.56	0.000
pDMN (13)	38.19	0.000
OFC (14)	21.74	0.000
iTEMP/FUS (15)	38.34	0.000
AMY/HIP (16)	50.55	0.000
PF (17)	17.35	0.000

Table S6: Test statistics corresponding to supplementary figure S6A: Results from two-sample t-tests comparing persistence control energy for normalized structural connectivity (streamline counts divided by the relative volume of the connected brain regions) for each iCAP between HCs and patients with 22q11DS. Age, gender and FSIQ were included as nuisance regressors. P-values were corrected for multiple comparisons based on permutation testing (Westfall and Young, 1993).

iCAP	T-statistic	p-value	effect size (Cohen's d)
dACC/dlPFC (1)	2.88	0.063	-0.50
LAN (2)	1.19	0.982	-0.50
FPN (3)	0.81	1.000	-0.50
PREC/vDMN (4)	-2.44	0.211	-0.50
VSN (5)	-1.23	0.974	-0.50
aDMN (6)	2.98	0.047	-0.50
secVis (7)	1.77	0.701	-0.50
PrimVis1 (8)	-0.18	1.000	-0.50
PrimVis2 (9)	-4.27	0.001	-0.50
aIN (10)	-2.82	0.073	-0.50
SM (11)	0.43	1.000	-0.50
AUD/SM (12)	-3.87	0.002	-0.50
pDMN (13)	2.53	0.173	-0.50
OFC (14)	-0.50	1.000	-0.50
iTEMP/FUS (15)	0.89	0.999	-0.50
AMY/HIP (16)	-1.59	0.825	-0.50
PF (17)	-0.42	1.000	-0.50

Table S7: Test statistics corresponding to supplementary figure S7: Results from two-sample t-tests comparing degree (total streamline count per region) of each iCAP between HCs and patients with 22q11DS. Age, gender and FSIQ were included as nuisance regressors. P-values were corrected for multiple comparisons based on permutation testing (Westfall and Young, 1993).

iCAP	t-statistic	p-value	effect size (Cohen's d)
dACC/dlPFC (1)	4.15	0.000	-0.67
LAN (2)	0.89	0.996	-0.14
FPN (3)	1.85	0.555	-0.30
PREC/vDMN (4)	1.97	0.461	0.32
VSN (5)	1.04	0.984	0.17
aDMN (6)	4.34	0.000	-0.71
secVis (7)	1.12	0.971	-0.18
PrimVis1 (8)	2.09	0.379	0.34
PrimVis2 (9)	4.93	0.000	0.80
aIN (10)	1.61	0.735	0.26
SM (11)	1.77	0.622	-0.29
AUD/SM (12)	2.75	0.085	0.45
pDMN (13)	0.04	1.000	0.01
OFC (14)	0.64	1.000	-0.10
iTEMP/FUS (15)	0.34	1.000	-0.06
AMY/HIP (16)	1.79	0.601	0.29
PF (17)	0.33	1.000	-0.05

Table S8: Test statistics corresponding to supplementary figure S9A: Results from two-sample t-tests comparing activation variability (i.e., the standard deviation of the time course) of each iCAP between HCs and patients with 22q11DS. Age, gender and FSIQ were included as nuisance regressors. P-values were corrected for multiple comparisons based on permutation testing (Westfall and Young, 1993).

iCAP	T-statistic	p-value	effect size (Cohen's d)
dACC/dlPFC (1)	2.73	0.097	-0.48
LAN (2)	2.34	0.250	-0.48
FPN (3)	2.59	0.141	-0.48
PREC/vDMN (4)	2.62	0.128	-0.48
VSN (5)	0.68	1.000	-0.48
aDMN (6)	4.39	0.000	-0.48
secVis (7)	-1.43	0.882	-0.48
PrimVis1 (8)	0.91	0.998	-0.48
PrimVis2 (9)	3.73	0.003	-0.48
aIN (10)	-1.51	0.839	-0.48
SM (11)	-3.09	0.031	-0.48
AUD/SM (12)	0.27	1.000	-0.48
pDMN (13)	2.28	0.289	-0.48
OFC (14)	-3.59	0.005	-0.48
iTEMP/FUS (15)	-5.95	0.000	-0.48
AMY/HIP (16)	-3.18	0.023	-0.48
PF (17)	-1.34	0.926	-0.48

Supplementary references

References

Karrer, T. M., Kim, J. Z., Stiso, J., Kahn, A. E., Pasqualetti, F., Habel, U., and Bassett, D. S. (2019). A practical guide to methodological considerations in the controllability of structural brain networks. *Journal of Neural Engineering*, in press:1–33.

Rubinov, M. and Sporns, O. (2010). Complex network measures of brain connectivity: Uses and interpretations. *NeuroImage*, 52(3):1059–1069. doi: 10.1016/j.neuroimage.2009.10.003.

Westfall, P. H. and Young, S. S. (1993). *Resampling-based multiple testing: Examples and methods for p-value adjustment*, volume 279. John Wiley & Sons.

Zöller, D., Sandini, C., Karahanoğlu, F. I., Padula, M. C., Schaer, M., Eliez, S., and Van De Ville, D. (2019). Large-Scale Brain Network Dynamics Provide a Measure of Psychosis and Anxiety in 22q11.2 Deletion Syndrome. *Biological Psychiatry: Cognitive Neuroscience and Neuroimaging*, 4(10):881–892. doi: 10.1016/j.bpsc.2019.04.004.